

Type Ia Supernovae from wide white-dwarfs triples

Erez Michaely¹[★]

¹*Astronomy Department, University of Maryland, College Park, MD 20742*

Accepted XXX. Received YYY; in original form ZZZ

ABSTRACT

For ultra-wide systems (with outer orbit $>10^3$ AU) the galactic field is collisional. Hence, ultra-wide triple white-dwarfs (TWDs) can be perturbed, by flyby stars, to sufficiently high outer eccentricity such that the triple becomes dynamically unstable. An unstable triple undergoes multiple binary-single resonant encounters between all three WDs. These encounters might result in a direct collision between any random two WDs and lead to a Type Ia supernova (SN) event. In case where the multiple resonant encounters did not produce a collision a compact binary is formed (while the third WD is ejected), this binary either collides or merges via gravitational wave emission, similar to the classic double-degenerate (DD) channel. In this research study we estimate the galactic rates of Type Ia SN from the direct collision channel to be $0.1\% - 4\%$ and primarily $2\% - 36\%$ from the DD scenario.

1 INTRODUCTION

One of the great open questions in astrophysics today is regarding the origin of Type Ia supernovae (SNe) (Maoz et al. 2014; Livio & Mazzali 2018; Soker 2019; Ruiter 2020). A type Ia SN is believed to be a thermonuclear explosion of a white-dwarf (WD) (Hoyle & Fowler 1960), however the channel or channels that lead to the explosion are under active research and debated frequently. SNe Ia are classified as such by a lack of hydrogen and helium lines in their spectra and by strong and wide lines of silicon, iron and calcium. Unlike core-collapse SNe (Smartt et al. 2009) which originate from massive (young) stars, thus only observed in star forming galaxies, Type Ia SNe are observed both in young (spiral galaxies) and old (elliptical galaxies) environments (Maoz et al. 2014).

Not all Ia SNe events are similar, there is a subclass of events named “peculiar SNe” which exhibits different characteristics. Their peak luminosity is usually lower than the standard events, like the 1991bg-like SNe; however, there were over-luminous cases observed, e.g. SN 1991T-like (Ruiter 2020). Peculiar SNe are hosted primarily in star forming galaxies and evolve faster than their “regular SNe” counterparts. In this manuscript we focus on regular Type Ia which are powered by the explosion of a carbon-oxygen (CO) WD.

There are several classical channels that aim to explain the evolution that lead to a Type Ia SN, we list them with no specific order.

The two popular theories are the single-degenerate (SD) and the double-degenerate (DD) theories. In the SD theory (Whelan & Iben 1973; Nomoto 1982) a CO WD accretes mass from a non-degenerate binary companion, sufficiently and effectively to reach the Chandrasekhar mass limit, and consequently explodes. In the DD theory (Iben & Tutukov 1984; Webbink 1984) two WDs coalesce through gravita-

tional wave (GW) emission. The merged product reaches the Chandrasekhar mass limit and explodes.

A third channel is the “core-degenerate” (CD) theory, where a degenerate WD merges with the hot core of an AGB-star, exceeds the Chandrasekhar mass limit and explodes when the core sufficiently cools (Kashi & Soker 2011; Ilkov & Soker 2012). A fourth channel is the “double-detonation” (DDet) (Woosley & Weaver 1994; Livne & Arnett 1995; Shen et al. 2018), in this sub-Chandrasekhar channel a WD accretes a layer of helium-rich material from a binary companion. The helium layer is ignited and detonates when compressed under the accreted material leading to a second detonation near the center of the CO WD. A recent scenario, fifth, describes the tidal disruption of a hybrid WD by a CO WD (Perets et al. 2019). Hybrid WDs are a natural outcome of binary stellar evolution and often overlooked as a possible source for Type Ia SNe. Similar to the DD theory, a hybrid WD can be tidally disrupted by the gravitational field of a close CO WD and form an accretion disk that detonates. All of the theories above present strong and weak points (Maoz et al. 2014; Tsebrenko & Soker 2015; Soker 2019) such that none of these theories are in consensus of the community.

The sixth and final theory we review here is the WD-WD collision scenario (2WDC) (Raskin et al. 2009; Thompson 2011; Katz & Dong 2012; Kushnir et al. 2013). In this scenario two WDs undergo direct collision, usually with a presence of a third companion and immediately ignite. The main strong point of this scenario is the well understood exploding mechanism (Kushnir et al. 2013) which is lacking from the other theories. However, this channel suffers from an extremely low merger rates (Toonen et al. 2018; Hamers et al. 2013; Prodan et al. 2013) and can explain $<0.1\%$ of observed SN rate.

In this paper we revisit this scenario and describe a new

channel that may explain up to 4% of the observed rate of Type Ia SNe from direct collisions and addition up to 36% from the new channel to the DD scenario.

Recently it was shown that for wide (semi-major axis $> 1000\text{AU}$) systems (either for binaries or triples) the field of the galaxy is collisional (Kaib & Raymond 2014; Michaely & Perets 2016, 2019b; Michaely & Perets 2020). During the lifetime of wide systems multiple gravitational interactions occur between the systems and a stellar flybys. This results in a change in the outer eccentricity of the outer binary, in the case of a triple or the eccentricity of the wide binary itself. Michaely & Perets (2016) showed that this may explain the formation of low-mass X-ray binaries, or gravitational waves sources from wide binary-BH in the field (Michaely & Perets 2019b) or recently from triple BH systems (Michaely & Perets 2020).

In this manuscript we mainly follow the dynamical treatment in Michaely & Perets (2020) and calculate the collision rate of two WD originating from initially wide triple systems.

This paper is organized as follows: In section 2 we describe the interaction of the triple in the field and calculate the fraction of systems that undergo the instability phase. In section 3 we treat the instability phase were multiple binary-single encounters occur, including the endstate. In section 4 we calculate the Type Ia SN rate for spiral and elliptical galaxies. Section 5 is dedicated to discussing the results and future work while we conclude the research in the summary in section 6.

2 FIELD WIDE WD TRIPLES

In the following we describe the impulse interaction between a random flyby star and a wide triple WD system in the field of the host galaxy. Similar mathematical description can be found in previous papers (Michaely & Perets 2016, 2019b; Michaely & Perets 2020). However, here we emphasize the main differences of this study from (Michaely & Perets 2020). Namely, the main goal in (Michaely & Perets 2020) is to calculate the merger rate of binary BH via gravitational wave emission, while here we focus on direct collision between two WDs. However, in section 4.2 we estimate the merger of two WDs via GW emission, similar to the standard DD scenario. We first describe the interaction in subsection 2.1 and treat the interaction in a quantitative way in section 2.2.

2.1 Qualitative description

It was previously shown by (Kaib & Raymond 2014; Michaely & Perets 2016, 2019b; Michaely & Perets 2020) that wide systems, either binaries or triples with outer semi-major axis (SMA), $a \gtrsim 1000\text{AU}$, interact with flyby stars sufficiently to change their pericenter distances, mainly through change in their eccentricity (Lightman & Shapiro 1977; Merritt 2013). This might lead to either a tidal interaction Michaely & Perets (2016), or inspiral due to GW emission (Michaely & Perets 2019b) or destabilize the triple (Michaely & Perets 2020). In this manuscript we focus on triple WDs (TWDs) in a wide and hierarchical configuration, where all the WD masses are equal; the inner binary is

constructed from two masses, m_1 and m_2 . The inner SMA is denoted by a_1 and the inner binary eccentricity is e_1 and is set to zero, for simplicity. The third WD, m_3 and the center of mass of the inner binary is considered as an outer binary with SMA, a_2 provided that $a_2 \gg a_1$. For illustration see Figure 1. One can relax the assumption that all three objects are WDs and estimate the collision rate of any triple that consists two WDs. However, this would be dominated by the collision of a WD with the third stellar companion, due to the size of the stellar companion with respect to a WD. This will be the focus of a future research.

Similar to (Michaely & Perets 2020) we are neglecting Lidov-Kozai oscillations effects (Lidov 1962; Kozai 1962; Naoz 2016; Michaely & Perets 2014). Here we focus on wide systems with $a_2 > 1000\text{AU}$. Therefore the Lidov-Kozai timescale is

$$\tau_{\text{LK}} \approx \frac{P_2^2}{P_1} \approx \quad (1)$$

$$6.6 \cdot 10^{13} \text{yr} \left(\frac{a_2}{10^4 \text{AU}} \right)^3 \left(\frac{a_1}{0.1 \text{AU}} \right)^{-\frac{3}{2}} \left(\frac{M}{1.8 M_\odot} \right)^{-1} \left(\frac{M_b}{1.2 M_\odot} \right)^{\frac{1}{2}}$$

where $M \equiv m_1 + m_2 + m_3$ is the total mass of the triple and $M_b \equiv m_1 + m_2$ is the total mass of the inner binary, τ_{LK} is larger than Hubble time.

A flyby interaction with wide systems can change the outer binary eccentricity in a way that the pericenter passage is inside the SMA of the inner binary, $q = a_2(1 - e_2) \lesssim a_1$. In this case, the triple becomes dynamically unstable (Stone & Leigh 2019; Samsing et al. 2014; Heggie 1975) and as a consequence the triple breaks down to a series of binary-single encounters, similar to the dynamics expected in dense environments even-though the triple resides in the field of the galaxy. In other words the dynamics of an unstable triple in the field is similar to the dynamics in dense environments.

There are two important timescales for flyby-triple interaction. First, the flyby-triple interaction timescale, $t_{\text{int}} \equiv b/v_{\text{enc}}$, where b is the closest approach of the stellar flyby to the center of mass of the triple system, and v_{enc} is the relative velocity at infinity of the stellar flyby compared to the center of mass of the triple. Second timescale is the orbital period of the outer binary, P_2 . Here, we consider only the impulsive interaction regime where $t_{\text{int}} \ll P_2$. In section 2.2 we calculate the rate where unstable triples are formed from hierarchical triples as a function of the inner and outer SMA.

During the dynamical instability phase multiple binary-single encounter occur. In every encounter a temporary binary is created with SMA, a' and eccentricity, e' . This binary is bounded to the third WD which orbits the center of mass of the temporary binary in a Keplerian orbit with timescale of t_{iso} (Michaely & Perets 2020). A fraction of all systems experience a direct collision between the two components of the inner temporary binary, $f_{\text{collision}}(a_1)$. We find $f_{\text{collision}}(a_1)$ in section 3.1.1.

2.2 Quantitative description

Consider an ensemble of hierarchical and wide TWDs. The masses of the WDs are equal $m_1 = m_2 = m_3 = 0.6 M_\odot$ (we denoted the total mass of the system by

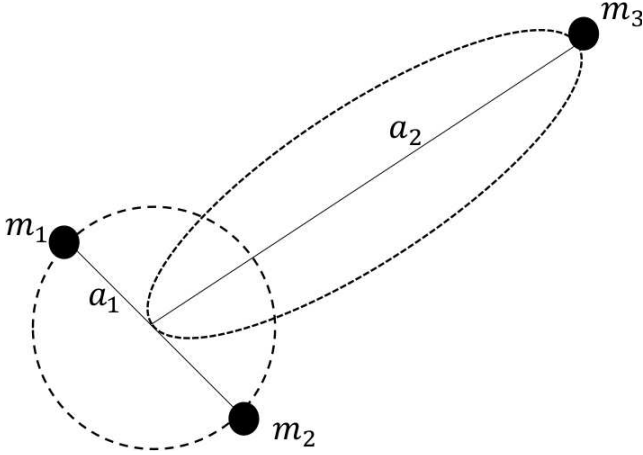


Figure 1. Cartoon of wide hierarchical TWD, $a_1 \ll a_2$. The inner binary orbit is circular. The outer binary eccentricity is drawn from a thermal distribution, $f(e_2) = 2e_2$.

M) the inner (outer) SMA a_1 (a_2). The distributions of a_1 and a_2 are log-uniform, $f_{a_{1(2)}} \propto 1/a_{1(2)}$ between $0.01\text{AU} - 100\text{AU}$ ($10^3\text{AU} - 10^5\text{AU}$). The inner binary is set to be circular, $e_1 = 0$ whereas the outer binary eccentricity is drawn from a thermal distribution, $f(e)de = 2ede$. All triples in the ensemble are embedded in the field with number stellar density of n_* and a velocity dispersion of σ_v which we set to be the relative velocity at infinity, v_{enc} .

Next we derive the fraction of the ensemble that, $q \leq a_1$. Namely, the third WD inside the SMA of the inner binary, and write it as a function of the outer SMA, a_2 and field number density, n_* . Moreover, we account for outer binary ionization from the random interaction with flyby stars.

The loss cone, F_q , is the fraction out of the systems in the ensemble that the $q \leq a_1$. The equality $q = a_1$ defines the critical eccentricity e_c where the system is marginally stable, namely

$$a_2 \cdot (1 - e_c) = a_1 \quad (2)$$

which corresponds to $e_c = 1 - a_1/a_2$.

$$F_q = \int_{e_c}^1 2ede = \frac{2a_1}{a_2}. \quad (3)$$

The loss cone is small, namely $F_q \ll 1$. If a TWD is in the loss cone, m_3 enters the inner binary within the outer orbital period, P_2 and a dynamical instability begins. Then the system is lost from the ensemble. Systems with eccentricities close to the critical eccentricities could potentially be perturbed to enter the loss cone and replenish it after the next flyby happens. In order to calculate what is the fraction of systems that are susceptible to enter the loss cone we calculate the smear cone. The smear cone is a measure in phase space that an outer binary can occupy after an impulsive interaction with a random flyby star. Defined by $\theta = \langle \Delta v \rangle / v_k$, where v_k is the relative Keplerian velocity between the components of the outer binary at the average separation, $\langle r \rangle = a_2 (1 + 1/2e^2)$. Because $F_q \ll 1$ we approximate $e \rightarrow 1$, namely $v_k = (GM/3a_2)^{1/2}$, where G is Newton's constant. The change in velocity $\Delta v \approx 3Ga_2m_p/v_{\text{env}}b^2$ (Hills 1981; Michaely & Perets 2019b) where m_p denotes the mass of the stellar flyby. Following (Michaely & Perets

2019b) we write can the smear cone

$$F_s = \frac{\pi\theta^2}{4\pi} = \frac{27}{4} \left(\frac{m_p}{M}\right)^2 \left(\frac{GM}{a_2v_{\text{enc}}^2}\right) \left(\frac{a_2}{b}\right)^4. \quad (4)$$

The fraction of the loss cone filled after a single flyby interaction is given by the ratio of the smear cone to loss cone:

$$\frac{F_s}{F_q} = \frac{27}{8} \left(\frac{m_p}{M}\right)^2 \left(\frac{GM}{a_2v_{\text{enc}}^2}\right) \left(\frac{a_2}{b}\right)^4 \left(\frac{a_2}{a_1}\right). \quad (5)$$

For the situation where the loss cone is continuously fill, $F_q = F_s$, the timescale of which systems are depleted is just the outer binary orbital period, P_2 . Therefore one can write the depletion rate, which is a function of the size of the loss cone to be

$$\dot{L}_{\text{Full}} = \frac{F_q}{P_2} \propto a_2^{-5/2} a_1 \quad (6)$$

notice that the depletion rate is independent of the local stellar density, n_* (the position in the galaxy) and scales with the inner binary SMA, a_1 . Hence the depletion rate is decreasing with wider outer SMA in the full loss cone regime.

In the case, where $F_s < F_q$, the loss cone is not completely full all the time. Namely for outer binaries with tighter orbits, which are less susceptible for eccentricity change from a random flyby interaction (4), we term this situation as the empty loss cone regime. In this case the depletion rate depends on the rate of systems being kicked into the loss cone. Specifically, $f = n_*\sigma v_{\text{enc}}$ where $\sigma = \pi b^2$ is the geometric cross-section of the random flyby interaction. In this case the timescale where the depletion occur is the timescale for entering the loss cone, namely $T_{\text{empty}} = 1/f$. We can find following this equation that f is just: (Michaely & Perets 2016, 2019b)

$$f = n_*\pi\sqrt{\frac{27}{8} \left(\frac{m_p}{M}\right)^2 \frac{GMa_2^4}{a_1}}. \quad (7)$$

When the two timescales are equal the rate where systems leave the loss cone is equal to the rate of systems entering the loss cone. The critical SMA that separates the full loss cone regime to the empty loss cone regime (where the timescales are equal (Michaely & Perets 2019b)) is given by

$$a_{\text{crit}} = \left(\frac{2}{27\pi^4} \frac{M}{m_p^2} \frac{a_1}{n_*^2}\right)^{1/7}. \quad (8)$$

Using a_{crit} we can calculate the fraction of systems that enter the loss-cone for the empty loss cone regime: $a < a_{\text{crit}}$, and for the full loss cone, $a > a_{\text{crit}}$. F_q is the loss fraction of systems in the ensemble after the relevant timescale, hence $(1 - F_q)$ is the fraction of the surviving systems. The relevant timescale for the empty loss cone regime is $T_{\text{empty}} = 1/f$. For the full loss cone regime that timescale is P_2 , the outer orbital period. Next we write the fraction of systems that enter the loss cone as a function of time, t as

$$L(a_1, a_2, n_*)_{\text{empty}} = 1 - (1 - F_q(a_1, a_2))^{t/f}. \quad (9)$$

For the limit $F_q t / T_{\text{empty}} \ll 1$ we can take the leading term to get the approximation

$$L(a_1, a_2, n_*)_{\text{empty}} = F_q t f \quad (10)$$

which is proportional to the size of the loss-cone, F_q , specifically

$$L_{\text{empty}} \propto F_q \propto a_2^{-1} a_1. \quad (11)$$

The loss fraction grows with SMA for $a_2 < a_{\text{crit}}$, unlike the full loss cone regime. This means that the highest lost fraction comes from TWD with SMA of a_{crit} . For the full loss cone we make the same treatment with

$$L(a_1, a_2, n_*)_{\text{full}} = 1 - (1 - F_q(a_1, a_2))^{t/P_2}, \quad (12)$$

and after expansion we get

$$L(a_1, a_2, n_*)_{\text{full}} = F_q t / P_2. \quad (13)$$

In the above mathematical treatment we ignored the disruption process for wide systems in collisional environments. Taking this into account by calculating the half-life time of the wide system from (Bahcall et al. 1985), where the half-life time is

$$t_{1/2} = 0.00233 \frac{v_{\text{enc}}}{G m_p n_* a_2} \quad (14)$$

accounting for the ionization process in the empty loss-cone we get

$$L(a_1, a_2, n_*)_{\text{empty}} = \tau F_q f (1 - e^{-t/\tau}) = \quad (15)$$

$$\tau \frac{2a_1}{a_2} n_* \pi \sqrt{\frac{27}{8} \left(\frac{m_p}{M}\right)^2 \frac{G M a_2^4}{a_1}} (1 - e^{-t/\tau}).$$

where $\tau = t_{1/2} / \ln 2$. While for the full loss-cone case:

$$L(a_1, a_2, n_*)_{\text{full}} = \tau \frac{F_q}{P_2} (1 - e^{-t/\tau}) = \quad (16)$$

$$\tau \frac{2a_1}{a_2} \left(\frac{GM}{4\pi^2 a_2^3}\right)^{1/2} (1 - e^{-t/\tau}).$$

As mentioned in previous work (Michaely & Perets 2020) the lost fraction is proportional to a_1 . A representative example of the loss probability, or the probability that a TWD becomes unstable due to flyby interactions is presented in figure 2.

In the next section we calculate the fraction of the cases where the triple becomes unstable and ends up as a Type Ia SN. This can happen either in a direct collision or a merger via GW emission.

3 INSTABILITY STAGE

When the triple enters the loss cone it becomes unstable. In the follow section we describe the dynamics this instability. Similar treatment is done in (Samsing et al. 2014, 2018; Michaely & Perets 2020).

The triple loses its hierarchy and as a consequence multiple binary-single encounters occur. The physics of binary-single encounters were studied mainly in the context of dense stellar environments, e.g. globular-clusters or galactic centers. A close binary-single interaction occurs when the single component passes within the binary sphere of influence. For a close binary-single interaction every gravitational force exerted between every pair of components is comparable in strength, hence the outcome is chaotic. Only two possible outcomes for the close binary-single interaction. First, direct-interaction, only one gravitational interaction takes place and the result is a binary, on a compact orbit and a single escaper. Second, intermediate state (IMS) or a resonant phase, where the triple turns to a temporary binary and

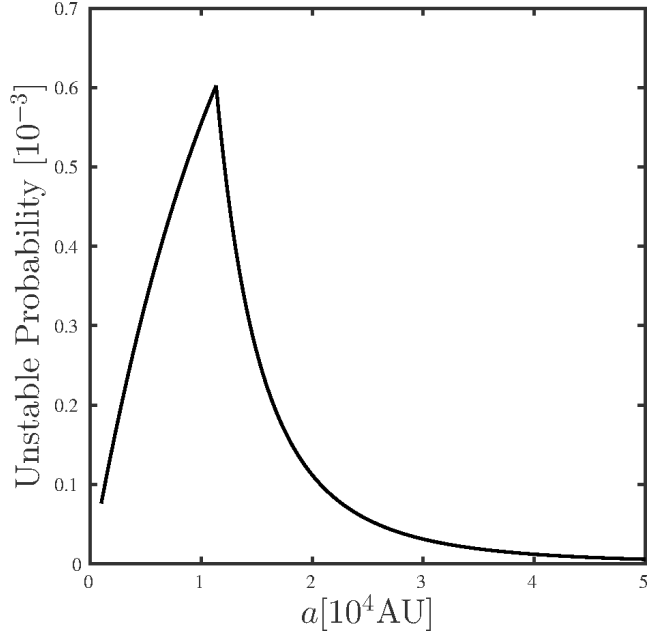


Figure 2. The probability for the triple to become unstable due to flyby interaction. Namely, the outer pericenter distance $q_2 = a_2 (1 - e_2) \leq a_1$. The plot is calculated for the following parameters: $t = 10\text{Gyr}$, $n_* = 0.1\text{pc}^{-3}$, $v_{\text{enc}} = 50\text{kms}^{-1}$. The highest probability is for a_{crit} . The full loss cone regime is for $a > a_{\text{crit}}$ and the empty loss cone regime is for $a < a_{\text{crit}}$.

a bound third object on a wide orbit. This happens multiple times ($\langle N_{\text{IMS}} \rangle = 20$), (Samsing & Ramirez-Ruiz 2017) for every binary-single encounter the orbital elements of both binaries (inner and outer) are drawn from the available distributions that conserve angular momentum and energy. The end-state of the multiple binary-single similar to the direct-interaction case, where a tight binary if formed, from any random two objects, and the third object escapes to infinity, an escaper.

From a direct collision perspective an event can occur either between scatters in the IMS or after the end-state is reached when the final binary escapes the gravitational potential of the third mass. In this study we calculate the merger rate only in the end-state case because we neglect the tiny fraction where the inner binary system losses enough orbital energy during the IMS to disconnect itself from the triple. In the following we calculate the rate of collisions in both cases and the merger rate from GW emission.

3.1 Intermediate state

Next we model the dynamics of the IMS, while in section 3.2 we describe the endstate in the post resonant phase. In this study we only consider WDs with equal masses of $0.6M_{\odot}$. The initial binary has a SMA, a_1 , and zero eccentricity. The single (third) WD interacts gravitationally with the inner binary, a close binary-single encounter. For each encounter a temporary binary is formed (with two random components out of the three WDs). The temporary binary eccentricity, e_{IMS} is drawn from thermal distribution and the SMA, a_{IMS} is determined by the energy budget which is approximated

by equation 12 in (Samsing et al. 2018)

$$\frac{m_1 m_2}{2a_1} = \frac{m_i m_j}{2a_{\text{IMS}}} + \frac{m_{ij} m_k}{2a_{\text{bs}}} \quad (17)$$

where a_{bs} is the temporary SMA of the outer binary. Where $\{i, j, k\}$ are the randomize indexes after the interaction and $m_{ij} = m_i + m_j$ is the mass of the temporary binary. From eq. (17) the outer SMA of the third bound WD can be written as

$$a_{\text{bs}} = a_1 \left(\frac{m_{ij} m_k}{m_1 m_2} \right) \left(\frac{a'}{a' - 1} \right) \quad (18)$$

where

$$a' \equiv \frac{a_{\text{IMS}}}{a_c} \text{ and } a_c \equiv a_1 \frac{m_i m_j}{m_1 m_2}. \quad (19)$$

In the equal mass case $a_c = a_1$ and therefore a' is just a_{IMS}/a_1 .

We write the lower and upper bound of a' . The lower bound of a' is trivial with

$$a'_L \approx 1, \quad (20)$$

while the upper bound should separate between the cases in the resonant state when the triple well described as a binary and a bound single, or when no temporary binary could be defined. This occurs, $a_{\text{bs}} \approx a_{\text{IMS}}$. Samsing et al. (2018) found that one way of estimating a'_U is by comparing the tidal force, F_{tid} exerts by the third BH to the binary gravitational binding force, F_{bin} . In the high eccentricity limit we find

$$F_{\text{tid}} \approx \frac{1}{2} \frac{G m_{ij} m_k}{a_{\text{bs}}^2} \frac{a_{\text{IMS}}}{a_{\text{bs}}} \quad (21)$$

$$F_{\text{bin}} \approx \frac{1}{4} \frac{G m_i m_j}{a_{\text{IMS}}^2}. \quad (22)$$

We set a'_U by the case that

$$\frac{F_{\text{tid}}}{F_{\text{bin}}} = 0.5 \quad (23)$$

which translates to

$$a'_U = 1 + \left(\frac{1}{2} \frac{m_k}{\mu_{ij}} \right)^{2/3} \quad (24)$$

where $\mu_{ij} \equiv m_i m_j / (m_i + m_j)$ is the reduced mass of the IMS binary.

The temporary inner SMA, a' values are distributed uniformly between a'_L and a'_U and the eccentricity distribution is thermal (Heggie 1975; Hut & Tremaine 1985; Rodriguez et al. 2018).

Given the temporary SMA, a' , and eccentricity, e' , one can calculate the pericenter $q' = a'(1 - e')$ and compare that to the combine radii of the two WD via the mass radius relation given by (Carroll & Ostlie 2006)

$$R_{\text{WD}} = 2.9 \times 10^8 \left(\frac{M_{\text{WD}}}{M_{\odot}} \right)^{-1/3} [\text{cm}], \quad (25)$$

where if $q' \leq 2R_{\text{WD}}$ we flag it as a direct collision. In the case where a collision did not occur we can calculate the orbital time of the third companion, t_{iso} . The orbital period is simply the Keplerian orbital period with a_{bs} , combining it with eq. (18) and eq. (19) we get:

$$t_{\text{iso}} = 2\pi \frac{a_1^{3/2}}{\sqrt{GM}} \left(\frac{m_{ij} m_k}{m_1 m_2} \right)^{3/2} \left(\frac{a'}{a' - 1} \right)^{3/2}. \quad (26)$$

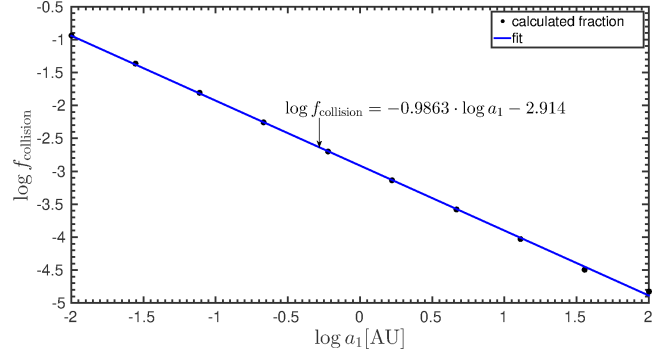


Figure 3. The fraction of systems, f_{collide} , that the inner binary collide during the resonant phase (IMS) as a function of the initial SMA, a_1 . For every a_1 we simulated 10^6 binary-single scattering experiments; for each experiment we use $N_{\text{IMS}} = 20$ scattering events in which we randomize the temporary binary orbital elements (see text) and check if this temporary IMS leads to a merger. Black dots, the calculated fraction for direct collision. Blue solid line, the fit to a power-law.

In section 3.2 we treat the case where no collision happen during the $\langle N_{\text{IMS}} \rangle$ scatters, and the end result is a compact binary and an escaper third object.

3.1.1 Estimating the collision fraction

We execute a numerical calculation to find the fraction of systems that the inner binary collides during the IMS as a function of a_1 . We sample 10 values of a_1 equally spaced in log from $(10^{-2} \text{ AU}, 10^2 \text{ AU})$. For each value of a_1 we randomize $N_{\text{tot}} = 10^6$ “scattering experiments”. These experiments are not N-body simulations, but Monte-Carlo approach. For each scattering experiment we set the number of binary-single encounters to be $N_{\text{IMS}} = 20$. For each encounter a temporary binary is created and bound to a third WD on a Keplerian orbit. The temporary binary orbital properties, a_{IMS} is drawn uniformly from (a'_L, a'_U) see equations (20) and (24), and the eccentricity, e_{ecc} is drawn from a thermal distribution. Next we calculate the temporary pericenter distance $q' = a'(1 - e')$ and compare it to the combine radii of the two WDs, $2R_{\text{WD}}$. If $q' \leq 2R_{\text{WD}}$ we count it as a collision and a source of Type Ia SN. If $q' > 2R_{\text{WD}}$ we calculate t_{iso} , to keep track on the time evolution and randomize the binary and single again, until we reach N_{IMS} times. In the case of no collision during the resonant phase we check the final end state, which have different orbital parameters distributions, see subsection 3.2. $f_{\text{collision}}(a_1)$ is the number of mergers divided by N_{tot} . The results are presented in Figure 3. We found a power law relation between $f_{\text{collision}}$ and a_1 , the exact fitted function is

$$f_{\text{collision}}(a_1) = 0.0114 \times a_1^{-0.954}. \quad (27)$$

3.1.2 Collision time

Here we show that a collision during the instability phase happens quickly, on a dynamical timescale, with respect to the evolution time. Therefore, one can ignore the time elapsed since the beginning of the instability phase until a direct collision occurs between two of the WDs. In figure 4

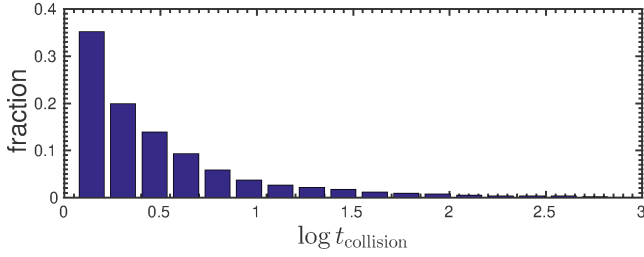


Figure 4. The collision time from the onset of the dynamical instability. The collision times are all much shorter than the interaction time t_{enc} therefore one can treat any collision as prompt with the turn of the triple to be unstable.

we show the distribution of collision time since the beginning of the resonant stage, it is evident from the figure that, unsurprisingly, the collision happens within ~ 1000 yrs since the first binary-single encounter, hence for the rest of the paper we consider a collision (i.e. SN) promptly when the system enters the instability stage.

3.2 Collision in the post-resonance phase

Here we describe the endstate of the resonant interaction where a tight binary is formed, with a SMA smaller than the initial one, $a_{\text{ES}} < a_1$ and a single WD escapes the system. It was previously shown in (Stone & Leigh 2019; Samsing et al. 2014; Heggie 1975) that the binary energy distribution scales like

$$E_{\text{ES}} \propto |E_1|^{-4} \quad (28)$$

where E_{ES} is the energy of the endstate binary and $E_1 = -Gm_1m_2/(2a_1)$ is the energy of the initial binary. Additionally, the endstate eccentricity, e_{ES} is drawn from thermal distribution (Stone & Leigh 2019). Therefore, for every system that did not collide during the IMS an endstate binary is formed with a_{ES} (E_{ES}) and e_{ES} . This binary either experiences a direct collision or merges through GW emission. In figure 5 we present the fraction of systems that collide in the post-resonance phase as a function of the initial SMA. The numerical fit presented in the figure is a broken power law

$$f_{\text{ES, coll}} = 1.52 \cdot 10^{-4} \times a_1^{-0.9393} \quad (29)$$

4 SN RATES

In what follows we calculate the SN rate from wide systems. In subsection 4.1 we calculate the Type IA SN rates originating from TWD systems via direct collisions. In section 4.2 we calculate the rates of DD mergers via GW emission for the endstate of the instability phase.

4.1 Type Ia SN rates from TWDs

In section 2.2 we describe the probability of a wide triple becomes unstable due to interaction with flyby stars. This probability depends on the local stellar environment through the local stellar density, n_* and the local velocity dispersion which sets the encounter velocity, v_{vec} . Therefore the host

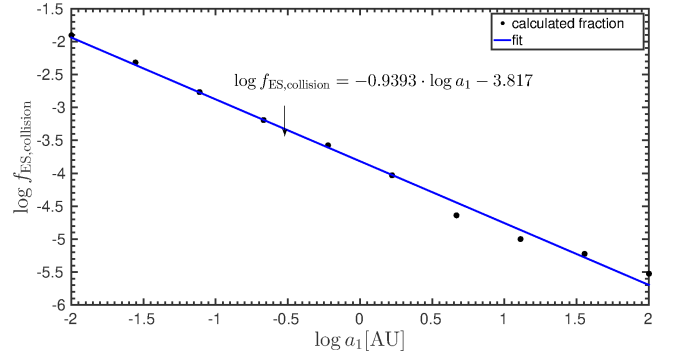


Figure 5. The fraction of systems that collide at the endstate of the chaotic dynamics, $f_{\text{EX, collide}}$ as a function of the initial SMA, a_1 . For every a_1 we simulated 10^6 binary-single scattering experiments; Black dots, the calculated fraction for direct collision. Blue solid line, the fit to a power law.

galaxy characteristics plays an important role in the SN rates from this channel.

We model two type of galaxies, spiral and elliptical. For the spiral galaxy we take the Milky-Way (MW) to represent all star forming galaxies.

Let

$$dN_s(r) = n_{*s}(r) \cdot 2\pi \cdot r \cdot h \cdot dr \quad (30)$$

(Michaely & Perets 2016) be the total number of stars in a galaxy region dr with scale height h . This region of the galaxy is located at distance r from the center. The galactic stellar density is modeled by the following function

$$n_{*s}(r) = n_0 e^{-(r-r_\odot)/R_l} \quad (31)$$

n_{*s} is the local stellar density for *spiral* galaxy and $n_0 = 0.1 \text{ pc}^{-3}$ is the stellar density in the solar neighborhood, $R_l = 2.6 \text{ kpc}$ (Jurić et al. 2008) is the galactic length scale. The mass of the flyby is taken to be $0.6 M_\odot$, the average stellar mass in the galaxy. The velocity dispersion is chosen to be the velocity dispersion of the flat rotation curve of the galaxy, $\sigma = 50 \text{ km s}^{-1}$.

For an elliptical galaxy model we take density profile from (Hernquist 1990) and translate it to stellar density given an average stellar mass of $0.6 M_\odot$.

$$n_{*e}(r) = \frac{M_{\text{galaxy}}}{2\pi r} \frac{r_*}{(r + r_*)^3} \quad (32)$$

where n_{*e} is the stellar density for *elliptical* galaxy and $r_* = 1 \text{ kpc}$ is the scale length of the galaxy, $M_{\text{galaxy}} = 10^{11} M_\odot$ is the total stellar (and not total) mass of the galaxy. Therefore

$$dN_e(r) = \frac{n_{*e}}{\langle m \rangle} dV \quad (33)$$

is the number of stars inside a local volume dV are a distance r from the center and $\langle m \rangle$ is the average stellar mass of the galaxy. The velocity dispersion for a typical elliptical galaxy is $\sigma = 160 \text{ km s}^{-1}$. Figure 6 shows the stellar density of the two prototypes of galaxies.

Now we estimate the fraction of TWDs out of the stellar population, f_{TWD} . We assume all stars with mass in the range of $1 M_\odot - 8 M_\odot$ become WDs. Given the Kroupa initial mass function (Kroupa 2001) a fraction of $f_{\text{primary}} \approx 0.1$ out of all stars are in the range of $1 M_\odot - 8 M_\odot$, e.g. will

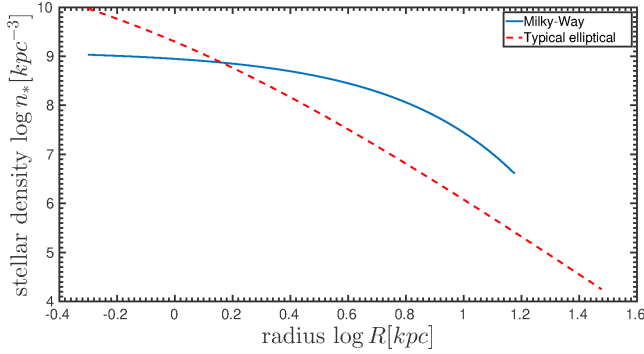


Figure 6. Number stellar density as a function of distance. The blue solid line represents the Milky-Way galaxy. The red dashed line represents a typical elliptical galaxy. Figure taken from [Michaely & Perets \(2020\)](#)

evolve to become WDs in 10Gyrs and actually less than that when accounting for binary stellar evolution. In order to estimate the binary companion mass we use uniform mass ratio distribution ([Moe & Di Stefano 2016](#)), $Q_{\text{inner}} \in (0.1, 1)$. For the third star we define the outer mass ratio $Q_{\text{outer}} = m_3 / (m_1 + m_2)$ and its value is distributed from a power law distribution ([Moe & Di Stefano 2016](#)) $f_{Q_{\text{outer}}} \propto Q_{\text{outer}}^{-2}$ and $Q_{\text{outer}} \in (0.1, 1)$, which is similar to random pairing to the initial mass function. Given these distributions we get that the fraction of secondaries in the range of producing WDs is $f_{\text{secondary}} \approx 0.45$, for the tertiaries is $f_{\text{tertiary}} \approx 0.42$. The fraction of triples is chosen to be $f_{\text{triple}} = 0.2$ and the fraction of wide outer binaries greater than 1000AU from a log-uniform distribution, f_{a_2} , is $f_{\text{wide}} = 0.2$. Combining these estimations we get

$$f_{\text{TWD}} = f_{\text{primary}} \times f_{\text{secondary}} \times f_{\text{tertiary}} \times f_{\text{triple}} \approx 3.8 \times 10^{-3} \quad (34)$$

out of which only f_{wide} are in wide configuration, hence

$$f_{\text{model}} = f_{\text{TWD}} \times f_{\text{wide}} = 7.6 \times 10^{-4} \quad (35)$$

is the fraction of the stellar population in a wide TWD configuration.

We note here, and expand in the discussion, that this is a simplification of a very complex estimation. In order to correctly calculate the wide TWD systems out of a certain stellar population one need to consider both single and binary stellar evolution. This would modify the initial SMA and eccentricity distributions whilst change the masses. Specifically, common envelope evolution ([Ivanova et al. 2013](#)) modifies the inner SMA and even the outer SMA due to mass loss from the inner binary ([Michaely & Perets 2019a; Igoshev et al. 2020](#)).

Next we calculate the total SN rate for the MW-like galaxy and an typical elliptical galaxy. The rate, Γ is given by integrating the loss cone (15) and (16) for all outer SMAs, a_2 between $10^3 - 10^5$ AU, the local stellar density in the galaxy n_* from equations (31) and (32). In order to integrate the inner binary SMA we use the following limits $10^{-2} (10^{-1}) - 10^2$ AU:

$$\Gamma = \int \int \int \frac{L_{\text{collision}}(a_1, a_2, n_*)}{10\text{Gyr}} da_1 da_2 dN(r) \quad (36)$$

where $L_{\text{collision}} \equiv L(a_1, a_2, n_*) f_{a_1} f_{a_2} f_{\text{model}} f_{\text{collision}}$ and we

define

$$dL \equiv \frac{L_{\text{collision}}(a_1, a_2, n_*)}{10\text{Gyr}} da_1 da_2 dN(r), \quad (37)$$

and write the integral for the MW-like galaxy

$$\Gamma_{\text{MW}} = \int_{0.5\text{kpc}}^{15\text{kpc}} \int_{10^3\text{AU}}^{10^5\text{AU}} \int_{10^{-2}(10^{-1})\text{AU}}^{10^2\text{AU}} dL \approx 2 (0.1) \times 10^{-5} \text{yr}^{-1} \quad (38)$$

and for a typical elliptical

$$\Gamma_{\text{elliptical}} = \int_{0.1\text{kpc}}^{30\text{kpc}} \int_{10^3\text{AU}}^{10^5\text{AU}} \int_{10^{-2}(10^{-1})\text{AU}}^{10^2\text{AU}} dL \approx 3.4 (0.2) \times 10^{-5} \text{yr}^{-1}. \quad (39)$$

These results are averaged on a 10Gyr lifetime of the galaxies, in section 5.1.2 we discuss the delay-time distribution of these collision.

In the case where a direct collision did not occur during the IMS phase the triple is disrupted and a compact binary is formed. We calculate the collision rate by using, $f_{\text{ES,col}}$ from (29) instead of $f_{\text{collision}}$ to get a SN rate for the MW-like galaxy

$$\Gamma_{\text{ES,MW}} = \int_{0.5\text{kpc}}^{15\text{kpc}} \int_{10^3\text{AU}}^{10^5\text{AU}} \int_{10^{-2}(10^{-1})\text{AU}}^{10^2\text{AU}} dL \approx 2 (0.12) \times 10^{-6} \text{yr}^{-1} \quad (40)$$

and for the elliptical galaxy a rate of

$$\Gamma_{\text{ES,elliptical}} = \int_{0.1\text{kpc}}^{30\text{kpc}} \int_{10^3\text{AU}}^{10^5\text{AU}} \int_{10^{-2}(10^{-1})\text{AU}}^{10^2\text{AU}} dL \approx 3.4 (0.21) \times 10^{-6} \text{yr}^{-1}. \quad (41)$$

The total rate for the case of $a_1 \in (10^{-2} (10^{-1}) \text{AU}, 10^2 \text{AU})$, over a galactic lifetime is for MW-like galaxy is $\sim 2.2 (0.11) \times 10^{-5} \text{yr}^{-1}$ and for elliptical galaxies $\sim 3.8 (0.22) \times 10^{-5} \text{yr}^{-1}$. Comparing that to the observed rate over the lifetime of a typical galaxy 10^{-3}yr^{-1} this channel may explain $\sim 0.1 - 2\%$ of all type Ia SNe in MW-like galaxies and $\sim 0.2 - 4\%$ in elliptical galaxies.

We note here and expand in the discussion that the uncertainty in expected collision rate, hence SN rate, is due to the uncertain structure of the triple systems, specifically the inner binary SMA distribution. The common envelope evolution may change the distribution of the SMA or even cause the inner binary itself to merge.

4.2 Mergers in the post-resonance phase

In the case where no direct collision occurred in the instability stage and imminently after the break-up of the triple into a compact WD binary and an escaper WD. We are left with two WD in a relatively close binary and eccentricity. These binaries omit GW and spiral in to eventually merge similarly to the classical DD scenario. Here we calculate the rate of these occurrences.

The merger timescale via GW emission for eccentric binaries is given from ([Peters 1964](#))

$$t_{\text{merger}} \approx \frac{768}{425} T_c(a) (1 - e^2)^{7/2} \quad (42)$$

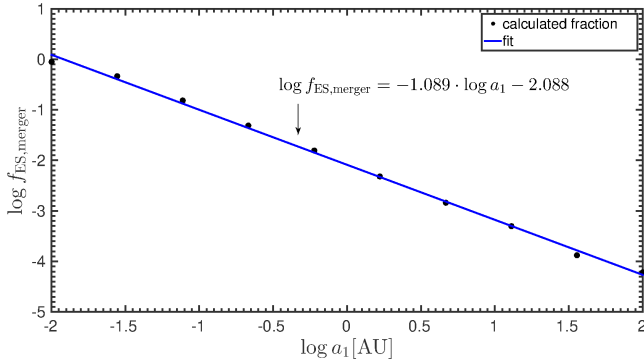


Figure 7. The fraction of systems that merge within 10^{10} yr at the endstate of the chaotic dynamics, $f_{\text{ES,merger}}$ as a function of the initial SMA, a_1 . For every a_1 we simulated 10^5 binary-single scattering experiments; Black dots, the calculated fraction of end-state mergers from our numerical experiment. Blue solid line, the best fit to a power law.

where $T_c = a^4/\beta$ is the merger timescale for a circular orbit and $\beta = 64G^3 m_i m_j (m_i + m_j) / (5c^2)$. Here $m_{i/j}$ are the indexes of the random two WDs that ended up as the surviving compact binary and c is the speed of light. If $t_{\text{merger}} < 10^{10}$ yr we flag this systems as a DD inspiral.

In figure 7 we present the calculated fraction of DD merger in the post-resonance phase. We found a broken power-law fit to the merger fraction

$$f_{\text{ES,merger}} = 0.008 \times a_1^{-1.089}. \quad (43)$$

Equipped with the functional form of the merger fraction we plug these in equation (36) to get the following rate for both types of galaxies and initial conditions:

$$\Gamma_{\text{ES,MW}} = \int_{0.5\text{kpc}}^{15\text{kpc}} \int_{10^3\text{AU}}^{10^5\text{AU}} \int_{10^{-2}(10^{-1})\text{AU}}^{10^2\text{AU}} dL \approx 2.2 (0.1) \times 10^{-4} \text{yr}^{-1} \quad (44)$$

and for the elliptical galaxy

$$\Gamma_{\text{ES,elliptical}} = \int_{0.1\text{kpc}}^{30\text{kpc}} \int_{10^3\text{AU}}^{10^5\text{AU}} \int_{10^{-2}(10^{-1})\text{AU}}^{10^2\text{AU}} dL \approx 3.6 (0.16) \times 10^{-4} \text{yr}^{-1} \quad (45)$$

Which account for $\sim 1 - 36\%$ of the Type Ia rates. This is an addition to the classical DD rate because these systems originate from binaries that their GW inspiral time is greater than Hubble time.

5 DISCUSSION

5.1 Model assumptions

The mathematical model and calculation we present here is based on several assumptions, in the following we address them.

WD masses. In this manuscript we use WD mass of $0.6M_\odot$ this is a simplification of single stellar evolution. Different WD masses correspond to different WD radii via the mass radius relation (25) and therefore different cross-section for a direct collision. Additionally, if the triple

consists of significantly different masses the assumption of $N_{\text{IMS}} = 20$ breaks down and a different treatment should be done. Moreover, different WD masses correspond to different triple evolution timescale. The importance of this issue is with regarding of the interaction of the triples with flybys during the MS lifetime, and with the time where actually the TWD is formed. A dedicated population synthesis will shed light on these issues.

Triple fraction and orbital elements. A key ingredient in this model in order to calculate the SN rate is the fraction of triple systems out of the stellar population, f_{model} and the distributions of the SMAs and eccentricities. The fractions we use in order to estimate f_{model} are taken from Moe & Di Stefano (2016) which describe MS binary stars and not WD binaries. The same holds for the SMA and eccentricity distributions which are motivated from the MS systems.

Single and binary stellar evolution effect both the SMA and eccentricity for each system. Mass-loss due to stellar evolution (slow mass-loss) leads to the expansion of the system's SMA while keeping the eccentricity constant. However, complex binary interaction, e.g. tidal interaction, mass transfer, CEE, might change both the SMAs and the inner and outer eccentricity considerably and might even disrupt the binaries (Michaely & Perets 2019b; Michaely & Perets 2020). As we present in section 4.1 the uncertainty in the SN rate is primarily effected by the inner SMA distribution and the lower boundary of the inner SMA, which is a result of CEE. In a future study we intend to account for the dynamics described here with a population synthesis study that account for these interaction in order to get a more accurate description of the SN rates.

5.1.1 Two WDs in a triple system

In this study we focused on TWD. A complementary fraction of the population is a triple system with two WDs and a low mass stellar companion, $< 1M_\odot$. In these systems the dynamics are similar with the scenario presents here because the third star have to be a low mass stellar companion hence similar in mass with the other two WDs. The only difference is that the low mass stellar companion radius is orders of magnitude greater than the WD radius. Therefore, the most probable outcome of the resonant phase is a direct collision between a WD and the low mass star. This collision occurs in the presence of a bound WD in a wide and eccentric orbit. This interesting scenario is not studied here and will be studies elsewhere.

5.1.2 Delay time distribution (DTD)

An important observable of Type Ia SNe is the DTD, dN/dt . The DTD is the hypothetical rate of Type Ia SNe that follows a quick star formation. It have been well established that the observed DTD is proportional to $1/t$ where t is the time since star formation (Maoz et al. 2014). In this section we try to estimate the DTD profile of the dynamical scenario described here.

The DTD is governed by the numbers of available systems to collide as a function of time. This in turn is a function of the initial mass function and the stellar evolution

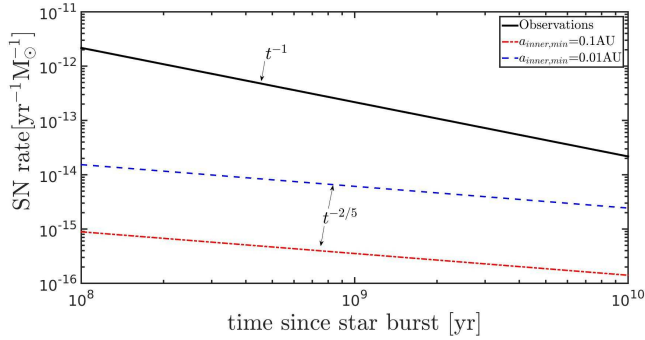


Figure 8. The delay-time distribution. Black solid line is the observed DTD, corresponds to a 10^{-3}yr^{-1} SN rate for a $10^{10}M_{\odot}$ galaxy. Blue dashed line is the estimated DTD for the 2WDC channel described here for the upper rate of $3.8 \times 10^{-5}\text{yr}^{-1}$ while the Red dashed-dot line is the DTD of the lower rate of $2.2 \times 10^{-6}\text{yr}^{-1}$. These DTD are calculated while ignoring the wide binary ionization process (described in the text) therefore should be treated as a upper limit.

time for each mass. Additionally, as stated in previous work, the rate of flyby interaction is constant in time if one disregards binary ionization. Therefore we can write the following dependency

$$\frac{dN}{dt} \propto \frac{dN}{dm} \frac{dm}{dt}. \quad (46)$$

In order to estimate the first term, we examine the star with lowest mass in the initial triple. This star will be the last to turn into a WD, hence determines the time since start formation where the TWD is formed. Given the population we simulated in 4.1 in order to calculate the triple fraction out of a given stellar population, one can find that the lowest stellar mass in a TWD progenitor scale with stellar mass, $dN/dm = m^{-2.75}$. This is steeper than for both Kroupa and Salpeter (Kroupa 2001; Salpeter 1955) IMFs. The second term is just the MS life time, t_{MS} , i.e. the time that takes a MS star evolve into a WD, $dm/dt = t^{-4/3}$. For these simplifying assumption we get

$$\frac{dN}{dt} \propto t^{2.75/3} t^{-4/3} = t^{-0.41} \approx t^{-2/5}. \quad (47)$$

As mentioned above the observed DTD of Type SNe is t^{-1} , this implies the as time progress the relative importance of the 2WDC channel increases and for late times this channel dominate over other channel see figure 8. After 10^{10}yr roughly up to 10% of all Type Ia SNe originate from the collision channel. We emphasize that in this calculation we neglected the ionization of wide binaries due to flyby interaction in the field. Equation (14) shows the complex dependencies of the ionization of a wide binary, specifically the SMA, a and the local stellar density. Therefore, one should treat figure 8 as an upper limit due to ionizations in later time as seem in equations (15) and (16).

5.2 Collisions and mergers from wide WD binaries

One can imagine a scenario where two WDs collide from a wide binary configuration. This scenario is far less efficient because the loss cone in the binary case, $F_{q,2}$ is orders of

magnitude less than the loss cone in the triple case, $F_{q,3}$ (3):

$$F_{q,2} = \frac{2R_{\text{WD}}}{a_2} \sim \frac{4 \times 10^{-5}\text{AU}}{10^4\text{AU}} \ll \frac{2 \times 10^{-1}\text{AU}}{10^4\text{AU}} = \frac{2a_1}{a_2} = F_{q,3}. \quad (48)$$

However, binaries one order of magnitude more frequent than triples therefore we find interest in calculating their rate in the future.

Moreover, similar to the scenario presented in (Michaely & Perets 2019b), the binary eccentricity can be excited to sufficiently high values so that the GW merger time, $t_{\text{merger}}(a, e)$, is shorter than the time between stellar encounters, t_{enc} . The time between encounter timescale is given by (Michaely & Perets 2019b)

$$t_{\text{enc}} = \frac{1}{f} = (n_* \sigma v_{\text{enc}})^{-1}. \quad (49)$$

For this channel, the loss cone is

$$F_{q,\text{GW}} = \left(\frac{\beta t_{\text{enc}}}{a_2^4} \right)^{-1}. \quad (50)$$

We will dedicate a future research for wide binary WDs are source for Type Ia SNe for completeness, and wide binaries consist of WD and a stellar companion as a source of cataclysmic variables.

6 SUMMARY

In this manuscript we explore the dynamical channel in which a TWD becomes dynamically unstable due to interactions with field stars. As a results the previously stable triple acts chaotically and experiences multiple binary-single encounters. In every such encounter there is a chance that the temporary inner binary would collide and result as a Type Ia SN. In the case where the triple survives the multiple binary-single encounters, the systems breaks down to a compact binary and an escaper WD. The compact binary either collide on its first orbit or merge via GW emission in much later time. If the inspiral time is shorter than the Hubble time, this system will merge, similar to the DD scenario.

We find that this dynamical channel that leads to a two WDs collision, may explain 2 – 36% of the observed Type Ia rates from the merger of two WDs and .1 – 4% from the direct collision channel, with the following caveats: the uncertainty of the inner binary evolution and the ionization of the outer binary. In this study we neglected the issue of the morphology of the remnant which is observed to be rather spherical in close by SN remnants and not yet well predicted in the 2WDC models.

ACKNOWLEDGMENTS

EM thanks Todd Thompson for enlightening comments, Hagai Perets and Noam Soker for interesting discussions together with the CTC (center of theory and computation) of the University of Maryland for financial support.

Data availability The data underlying this article will be shared on reasonable request to the corresponding author.

REFERENCES

- Bahcall J. N., Hut P., Tremaine S., 1985, *ApJ*, **290**, 15
- Carroll B. W., Ostlie D. A., 2006, *An introduction to modern astrophysics and cosmology*
- Hamers A. S., Pols O. R., Claeys J. S. W., Nelemans G., 2013, *MNRAS*, **430**, 2262
- Heggie D. C., 1975, *MNRAS*, **173**, 729
- Hernquist L., 1990, *ApJ*, **356**, 359
- Hills J. G., 1981, *AJ*, **86**, 1730
- Hoyle F., Fowler W. A., 1960, *ApJ*, **132**, 565
- Hut P., Tremaine S., 1985, *AJ*, **90**, 1548
- Iben I. J., Tutukov A. V., 1984, *ApJS*, **54**, 335
- Igoshev A. P., Perets H. B., Michaely E., 2020, *MNRAS*, **494**, 1448
- Ilkov M., Soker N., 2012, *MNRAS*, **419**, 1695
- Ivanova N., et al., 2013, *A&ARv*, **21**, 59
- Jurić M., et al., 2008, *ApJ*, **673**, 864
- Kaib N. A., Raymond S. N., 2014, *ApJ*, **782**, 60
- Kashi A., Soker N., 2011, *MNRAS*, **417**, 1466
- Katz B., Dong S., 2012, *ArXiv*,
- Kozai Y., 1962, *AJ*, **67**, 591
- Kroupa P., 2001, *MNRAS*, **322**, 231
- Kushnir D., Katz B., Dong S., Livne E., Fernández R., 2013, *ApJ*, **778**, L37
- Lidov M. L., 1962, *Planet. Space Sci.*, **9**, 719
- Lightman A. P., Shapiro S. L., 1977, *ApJ*, **211**, 244
- Livio M., Mazzali P., 2018, *Phys. Rep.*, **736**, 1
- Livne E., Arnett D., 1995, *ApJ*, **452**, 62
- Maoz D., Mannucci F., Nelemans G., 2014, *ARA&A*, **52**, 107
- Merritt D., 2013, *Classical and Quantum Gravity*, **30**, 244005
- Michaely E., Perets H. B., 2014, *ApJ*, **794**, 122
- Michaely E., Perets H. B., 2016, *MNRAS*, **458**, 4188
- Michaely E., Perets H. B., 2019a, *MNRAS*, **484**, 4711
- Michaely E., Perets H. B., 2019b, *ApJ*, **887**, L36
- Michaely E., Perets H. B., 2020, *Monthly Notices of the Royal Astronomical Society*
- Moe M., Di Stefano R., 2016, preprint, ([arXiv:1606.05347](https://arxiv.org/abs/1606.05347))
- Naoz S., 2016, *ARA&A*, **54**, 441
- Nomoto K., 1982, *ApJ*, **253**, 798
- Perets H. B., Zenati Y., Toonen S., Bobrick A., 2019, arXiv e-prints, p. [arXiv:1910.07532](https://arxiv.org/abs/1910.07532)
- Peters P. C., 1964, *Physical Review*, **136**, 1224
- Prodan S., Murray N., Thompson T. A., 2013, arXiv e-prints, p. [arXiv:1305.2191](https://arxiv.org/abs/1305.2191)
- Raskin C., Timmes F. X., Scannapieco E., Diehl S., Fryer C., 2009, *MNRAS*, **399**, L156
- Rodriguez C. L., Amaro-Seoane P., Chatterjee S., Kremer K., Rasio F. A., Samsing J., Ye C. S., Zevin M., 2018, *Phys. Rev. D*, **98**, 123005
- Ruiter A. J., 2020, arXiv e-prints, p. [arXiv:2001.02947](https://arxiv.org/abs/2001.02947)
- Salpeter E. E., 1955, *ApJ*, **121**, 161
- Samsing J., Ramirez-Ruiz E., 2017, *ApJ*, **840**, L14
- Samsing J., MacLeod M., Ramirez-Ruiz E., 2014, *ApJ*, **784**, 71
- Samsing J., MacLeod M., Ramirez-Ruiz E., 2018, *ApJ*, **853**, 140
- Shen K. J., et al., 2018, *ApJ*, **865**, 15
- Smartt S. J., Eldridge J. J., Crockett R. M., Maund J. R., 2009, *MNRAS*, **395**, 1409
- Soker N., 2019, *New Astron. Rev.*, **87**, 101535
- Stone N. C., Leigh N. W. C., 2019, *Nature*, **576**, 406
- Thompson T. A., 2011, *ApJ*, **741**, 82
- Toonen S., Perets H. B., Hamers A. S., 2018, *A&A*, **610**, A22
- Tsebrenko D., Soker N., 2015, *MNRAS*, **447**, 2568
- Webbink R. F., 1984, *ApJ*, **277**, 355
- Whelan J., Iben I. J., 1973, *ApJ*, **186**, 1007
- Woosley S. E., Weaver T. A., 1994, *ApJ*, **423**, 371